

Journal of Materials Chemistry C

Accepted Manuscript



This is an *Accepted Manuscript*, which has been through the Royal Society of Chemistry peer review process and has been accepted for publication.

Accepted Manuscripts are published online shortly after acceptance, before technical editing, formatting and proof reading. Using this free service, authors can make their results available to the community, in citable form, before we publish the edited article. We will replace this *Accepted Manuscript* with the edited and formatted *Advance Article* as soon as it is available.

You can find more information about *Accepted Manuscripts* in the [Information for Authors](#).

Please note that technical editing may introduce minor changes to the text and/or graphics, which may alter content. The journal's standard [Terms & Conditions](#) and the [Ethical guidelines](#) still apply. In no event shall the Royal Society of Chemistry be held responsible for any errors or omissions in this *Accepted Manuscript* or any consequences arising from the use of any information it contains.

ARTICLE

Formation mechanism of CdSe QDs through the thermolysis of Cd(oleate)₂ and TOPSe in the presence of alkylamine[†]

Cite this: DOI: 10.1039/x0xx00000x

Taekeun Kim,^a Yun Ku Jung^a and Jin-Kyu Lee^{* a}

Received 00th January 2012,

Accepted 00th January 2012

DOI: 10.1039/x0xx00000x

www.rsc.org/

The thermal decomposition of Cd(oleate)₂, a metal organocarboxylate complex, in the presence of alkylamine was studied in order to understand the formation mechanism of CdSe nanocrystals (quantum dots, QDs) in the hot-injection method. The major intermediates and side products were characterized by nuclear magnetic resonance (NMR) spectroscopy, X-ray diffraction (XRD), and transmission electron microscopy (TEM). The results showed that the nucleophilic attack of the metal-coordinated amine toward the most electron-deficient carbonyl carbon of the oleate ligands initiated decomposition to generate a CdO cluster (or oligomer). Based on our experimental results, we proposed a two-step formation mechanism for CdSe QDs involving the formation of CdO intermediates with alkylamines playing a critical role as the nucleophiles in the thermolysis process, followed by a metathesis reaction with trioctylphosphine selenide (TOPSe) as a chalcogenide source.

Keywords: CdSe, quantum dot, thermolysis, formation mechanism, alkylamine

Introduction

Throughout the last several decades, semiconductor quantum dots (QDs) have attracted considerable attention from researchers due to their novel electronic and optical properties, which can be tuned by the quantum size effect. The synthesis and characterization of high quality QDs have been extensively investigated,^{1, 2} since L. E. Brus *et al.* first reported the size dependence of the excited electronic properties of semiconductor nanocrystals.³ The development of synthesis methods for semiconductor QDs has led to the use of synthetically convenient and safe chemicals, such as CdO, 1-octadecene, and single-molecule precursors.⁴⁻⁷ In addition, an improved understanding of the reaction kinetics of monomer formation prior to particle nucleation and shape evolution has enabled the synthesis of various types of quantum dots, rods, and tetrapods of CdSe as well as of core-shell structure QDs.⁸⁻¹⁰ Among the various synthesis methods, thermal decomposition processes have been extensively studied by numerous research groups because they allow facile control of shape and size and good crystalline products.¹¹⁻¹⁴

The mechanism of colloidal nanocrystal synthesis is thought to involve molecular precursors that react to produce active "monomers". Based on the traditional colloidal formation mechanism,¹⁵ the rapid formation of these monomers creates a highly supersaturated condition, which initiates the nucleation of clusters or very small nanocrystals, and the nucleated

particles grow by interparticle Ostwald ripening.¹⁵⁻¹⁷ However, this growth mechanism does not perfectly explain the conversion from precursors to nanocrystals and only addresses the size distribution and selective plane growth after seed formation. It is still not chemically understood how precursor molecules are decomposed or transformed to so-called active monomers; a better understanding of this process is necessary to successfully modify and optimize the synthetic method.

Bawendi *et al.* conducted the pioneering work and proposed a mechanism involving two possible pathways of [PbSe] monomer formation.¹⁸ According to their proposed mechanism, TOPSe can be regarded as a source of either Se⁰ or Se²⁻ because of the weak P-Se bond. In the first proposed pathway, TOPSe reacts directly with the Pb²⁺ center of a Pb(oleate)₂ complex to produce TOPO, oleate anhydride, and [PbSe] monomer. In the second proposed pathway, reduced Pb⁰ species from Pb²⁺ in the presence of a reducing agent (diphenylphosphine, DPP) react with Se⁰ that is delivered from TOPSe, resulting in the formation of [PbSe] monomer, anhydride and free TOP. Alivisatos *et al.* have carried out studies of CdSe formation in systems without reducing agents or nucleophilic materials and proposed a mechanism that was very similar to the formation mechanism of PbSe proposed by Bawendi *et al.*¹⁹ Recently, a number of studies have aimed at understanding the chemical mechanism of nanocrystal formation for organometallic precursors and tertiary phosphine selenide or secondary phosphine, suggesting either the direct reaction of tertiary

phosphine selenide with the metal center to generate CdSe, tertiary phosphine oxide, and anhydride or the reaction of active secondary phosphine selenide with the metal center.²⁰⁻²³ García-Rodríguez *et al.* recently suggested the mechanism that selenium is directly binding to cadmium in the presence of alkylamine. But, they mentioned that their mechanistic and kinetics studies were conducted at relatively low temperature (<110 °C).²⁴ We have also recently proposed a mechanism for the thermal decomposition of metal dialkyldithiocarbamate ($M(S_2CNR_2)_2$), a single molecule precursor for forming metal sulfide nanoparticles, in the presence of alkylamines;²⁵ the binding of amines to the metal center and migration to the thiocarbonyl carbon in the ligand molecule are the important steps that induce the decomposition of the intermediate complex to give rise to MS monomers, corresponding organic side products, and H₂S. Moreover, we have shown that this mechanism could be extended to the decomposition of metal alkylcarboxylate ($M(O_2CR)_2$) precursors to generate metal oxides particles.²⁵ Interestingly, the formation of CdSe QDs from the reaction between CdO and TOPSe has been reported. Xu *et al.* have reported that FePt@CdO core-shell intermediates were synthesized through a reaction between FePt nanoparticles and Cd(acac)₂ as the cadmium precursor to generate FePt@CdO. The subsequent addition of a chalcogenide source yielded FePt@CdX core-shell nanocrystals (X = Se or S).²⁶ Furthermore, Klubunde *et al.* have investigated a novel strategy to prepare CdSe QDs directly from commercially available CdO powder, TOPSe and TOP in a heterogeneous system without using any organic acids.²⁷ Therefore, it is possible that Cd(O₂CR)₂ is first decomposed to CdO monomers in the presence of a nucleophile (amine, in our case) and then reacts with TOPSe to generate CdSe QDs and TOPO in a stepwise mechanism.

Here, we show experimental results for the two-step mechanism based on the thermal decomposition of metal carboxylates ($M(oleate)_2$) in the presence of alkylamine playing a critical role as the nucleophile at 250 °C to generate the CdO cluster intermediates, followed by a metathesis reaction with trioctylphosphine selenide (TOPSe) to produce CdSe QDs.

Experimental details

Chemicals and Instrumentation: Cadmium oxide, zinc acetate, selenium powder, sulfur powder, TOPO, oleylamine, octylamine, oleic acid, 1-octadecene and the solvents (hexane, chloroform, toluene, and ethanol) were purchased from Aldrich. Trioctylphosphine (TOP, 97%) was purchased from Aldrich and vacuum distilled to remove dioctylphosphine impurities. NMR solvents (chloroform-*d*₁ and toluene-*d*₈) were purchased from CIL. All chemicals were used without further purification. UV-Vis and PL spectra were recorded by a Scinco S-3100 and Jasco FP-6500 spectrophotometer. X-ray powder diffraction measurements were carried out on D8 Advance (Bruker) and M18XHF-SRA (MAC Science Co.) instrument. Transmission electron microscopy (TEM) and energy-dispersive spectroscopy (EDS) were conducted using Hitachi-7600 (Hitachi) and JEM-3000F (JEOL) instruments, respectively. NMR spectra were recorded on Jeol JNM-LA400 (JEOL) and DPX 300 (Bruker) instruments. FAB-MS spectrometer (GC-MS) measurements were carried out on a JMS-700 (JEOL).

Synthesis of TOPSe: Elemental Se (0.7896 g, 10 mmol) with an excess amount of TOP (10 mL, 22.4 mol) was stirred in a

glove-box for 1 h at room temperature to generate a clear 1 M solution of TOPSe.

Synthesis of Metal Oleate Complexes ($M(oleate)_n$, M = Cd, Zn, Fe and Mn): The iron and manganese oleate complexes were synthesized by the following method reported in the literature.²⁸ In a typical synthesis, 40 mmol of iron(III) chloride (or manganese chloride) and 120 mmol of sodium oleate was dissolved in a mixed solvent of ethanol (80 mL), distilled water (60 mL), and hexane (140 mL). The resulting solution was heated at 70 °C for 4 h. When the reaction was complete, the upper organic layer containing the $M(oleate)_n$ was washed three times with 30 mL of distilled water using a separatory funnel. A waxy solid of the corresponding metal oleate complexes were obtained almost quantitatively after hexane was evaporated. For the synthesis of the cadmium and zinc oleate complexes, the mixture of cadmium oxide (or zinc acetate) (1.0 mmol) and oleic acid (3.0 mmol) was degassed at 100 °C and then heated to 180 °C to dissolve the cadmium oxide under N₂ gas. The products were isolated by precipitation using an excess amount of acetone to remove the remaining oleic acid.

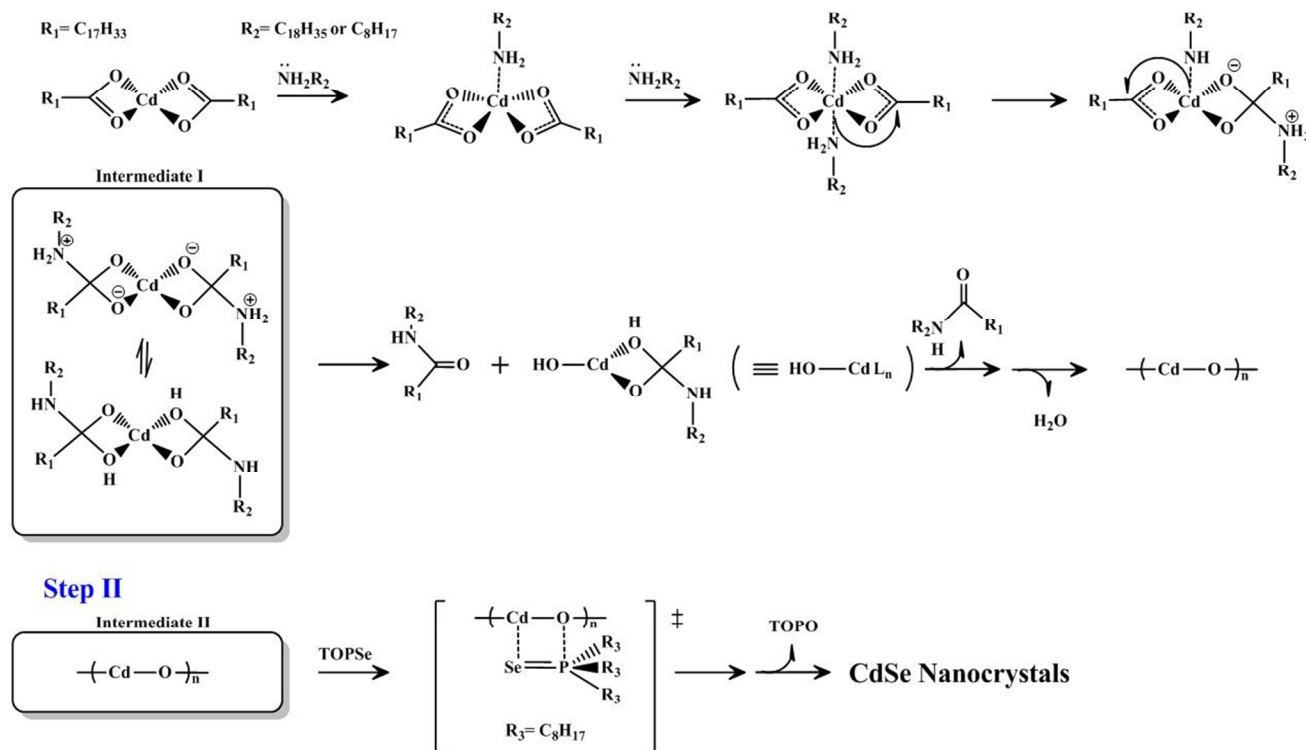
Thermal decomposition of $M(oleate)_n$ to generate metal oxide nanoparticles: A 1.0 mmol of $M(oleate)_n$ was added to the mixed solution of 1-octadecene (10 mL) and octylamine (4.0 mmol), and the mixture was heated to 270 °C with vigorous stirring (heating rate: 15 °C/min). When the reaction mixture turned opaque due to the formation of insoluble metal oxide nanoparticles during heating, the temperature was measured and designated as the decomposition temperature of the corresponding metal oleate complex. The mixture was then maintained at that temperature for 30 min to complete the reaction.

NMR experiments to monitor the generation of intermediate I from Cd(oleate)₂ and octylamine: Cd(oleate)₂ (1.0 mmol) and various amounts of octylamine (1.0~4.0 mmol) were mixed in 5 mL of toluene-*d*₈ at room temperature. The mixed solution was sealed in an NMR tube and heated for different periods of time. After cooling to room temperature, the supernatant was collected for use in NMR measurements.

Separation of CdO clusters (intermediate II): The 1-octadecene solution containing Cd(oleate)₂ (1.0 mmol) and octylamine (4.0 mmol) was degassed and then filled with N₂. The mixed solution was heated to 250 °C and then removed from the heating system. After cooling to room temperature, an excess amount (30 mL) of acetone was added to the mixture, and the generated precipitates were separated by centrifugation. The precipitated CdO clusters (intermediate II) were redispersed in hexane and collected by centrifugation.

Synthesis of CdSe QDs: CdSe QDs were synthesized by a method previously reported in the literature.²⁹ The 1-octadecene solution containing Cd(oleate)₂ (1.0 mmol) and octylamine (4.0 mmol) was degassed and then filled with N₂. The mixed solution was heated to 250 °C and TOPSe solution (1.0 mmol in TOP) was injected. As control experiments to confirm the mechanism, CdSe QDs were also synthesized by reacting 1.0 mmol of TOPSe with ~100 nm CdO nanoparticles (1.0 mmol) or bulk CdO powder (1.0 mmol) as well as with intermediate II (CdO cluster, the exact amount was not determined but much smaller than 1.0 mmol).

Step I



Scheme 1. Proposed thermal decomposition mechanism of Cd(oleate)₂ in the presence of alkylamine to form CdSe QDs in two steps: formation of intermediates I and II (Step I), and CdSe QDs formation from intermediate II and TOPSe (Step II)

Result and Discussion

The proposed reaction mechanism between Cd(oleate)₂ and TOPSe in the presence of alkylamine is divided into two steps, as described in Scheme 1. The first step is the thermal decomposition reaction of Cd(oleate)₂ facilitated by the alkylamine to generate the CdO cluster or oligomer, (CdO)_n, and the next step is the reaction of the CdO cluster with TOPSe to produce a CdSe nanoparticle.

To understand the interaction between alkylamine and the metal oleate precursors, Cd(oleate)₂ was mixed with 1, 2, or 4 eq. of octylamine in toluene-*d*₈, and the solutions were monitored by ¹H NMR at room temperature. As clearly shown in Fig. 1, the ¹H NMR spectra of these mixture solutions showed a representative peak from NH₂-CH₂-C₇H₁₅ at 2.85, 2.70, and 2.61 ppm when the amount of added amine was increased; these positions shifted downfield from that of the free octylamine (2.47 ppm) due to the coordination to the metal site of Cd(oleate)₂. This confirmed that the octylamine was not tightly bound to Cd(oleate)₂ in the solution but rather existed in a dynamic equilibrium state on the NMR time scale, showing an averaged chemical shift value between the coordinated and the free octylamines.

From the ¹H NMR spectra of the mixture solutions of Cd(oleate)₂ and octylamine, a new, low intensity peak at 3.37 ppm could be observed (Fig. 1b and 1c, and enlarged spectrum

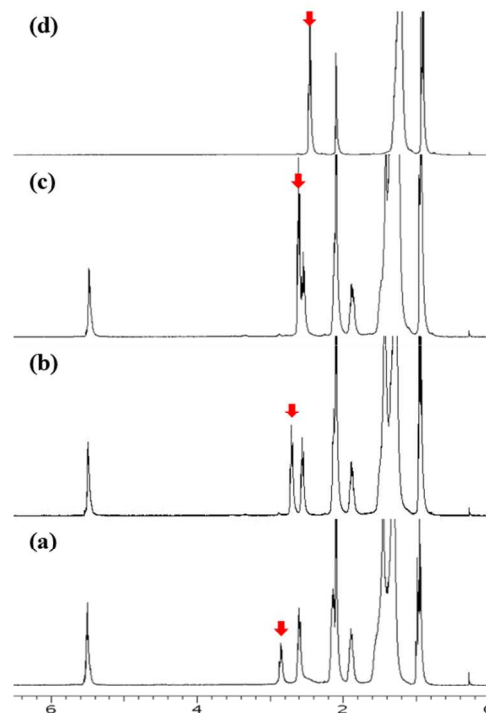


Fig. 1 ¹H NMR spectra; 1 eq. of Cd(oleate)₂ was mixed with (a) 1 eq., (b) 2 eq., and (c) 4 eq. of octylamine; (d) free octylamine in toluene-*d*₈

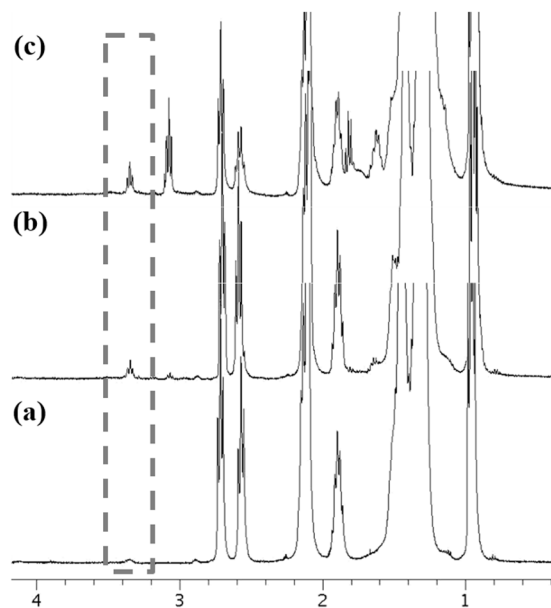


Fig. 2 The peak corresponding to $-\text{NH}_2^+-\text{CH}_2\text{C}_7\text{H}_{15}$ in the ^1H NMR spectra of intermediate I, generated from the reaction of $\text{Cd}(\text{oleate})_2$ and octylamine (1:2 ratio), gradually increased as the temperature was raised; (a) room temperature, (b) 150 °C, (c) 180 °C

In Fig. 2a). When the mixed solution (1:2 ratio) in the sealed NMR tube was kept at the higher temperature sand bath, the intensity of this peak increased, as shown in Fig. 2b and 2c. However, at 180 °C, the intensity did not increase significantly probably due to the instability of the generated intermediate, and other peaks at 3.10 began to appear; this peak could be assigned to the final side product of the thermal decomposition reaction, *N*-octyloleamide, which will be explained later in detail.

Furthermore, when the mixed solution (1:4 ratio) was refluxed in toluene- d_8 at 110 °C, the decomposition reaction proceeded slowly enough to be easily monitored by NMR (Fig. 3). The NMR spectra of the supernatant were collected after the solid product was removed by centrifugation from the mixed solution after refluxing for 0, 24, and 48 h. They clearly showed the disappearance of the peak from $\text{CH}_3(\text{CH}_2)_7\text{CH}=\text{CH}(\text{CH}_2)_6-\text{CH}_2\text{CO}_2$ in the coordinated oleate ligands (2.53 ppm) and the gradual shift of the peak from coordinated $\text{NH}_2\text{CH}_2\text{C}_7\text{H}_{15}$ at 2.60 to 2.45 ppm corresponding to free octylamine after 48 h, which appeared due to the consumption of $\text{Cd}(\text{oleate})_2$ during the decomposition reaction, which prevented octylamine binding. In addition, a new peak at 3.10 ppm appeared as the decomposition reaction proceeded, which could be assigned to the side product, *N*-octyloleamide, $\text{CH}_3(\text{CH}_2)_7\text{CH}=\text{CH}(\text{CH}_2)_6-\text{CH}_2\text{CO}_2\text{NH}(\text{CH}_2)_7\text{CH}_3$. Even after 48 h of refluxing, however, the decomposition reaction was not complete, based on the relative intensity of the peak at 3.10 ppm compared to that of the peak at 5.45 ppm, which corresponds to protons from the double bonds in the oleyl unit. Interestingly, the intensity of the peak at 3.37 ppm mentioned in Fig. 2 did not change significantly during the reaction at 110 °C as shown in Fig. 3. It was assumed that the peak at 3.37 ppm might belong to intermediate I, which was generated by the migration of the

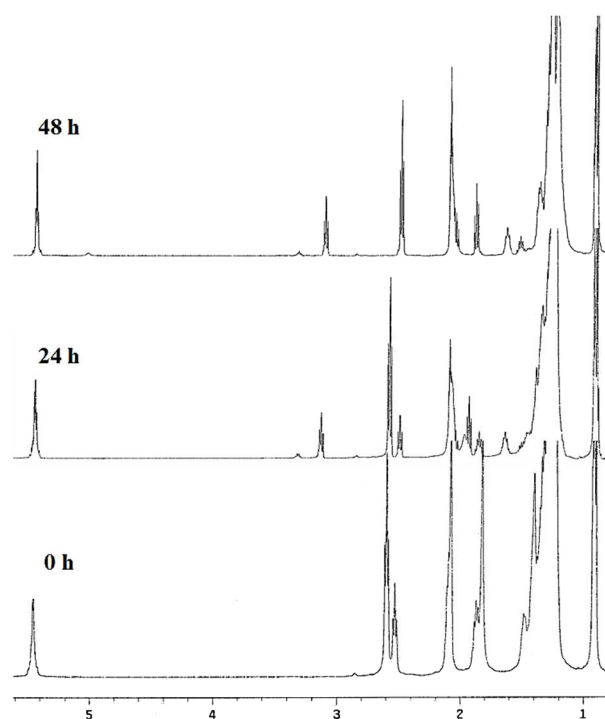


Fig. 3 ^1H NMR spectra of the mixture of $\text{Cd}(\text{oleate})_2$ with octylamine (1:4 ratio) in toluene- d_8 at 110 °C at different reaction times

coordinated amine to the oleate ligand. Intermediate I might not be stable at temperatures higher than 110 °C, giving rise to the final products of *N*-octyloleamide and $(\text{CdO})_n$ along with the generation of water, as described in Step I of the Scheme 1.

To confirm the generation of intermediate I by the migration of the coordinated octylamine to the most electronically deficient carbonyl carbon of the oleate ligand in the $\text{Cd}(\text{oleate})_2$ complex, similar to the result previously shown in the metal dialkyldithiocarbamate ($\text{M}(\text{S}_2\text{CNR}_2)_2$) case,²⁵ $\text{Cd}(\text{oleate})_2$ was mixed with 3 eq. of octylamine in toluene- d_8 and heated in a sealed NMR tube at 150 °C for 2 h, which was then cooled to room temperature for ^1H NMR analysis. The two-dimensional (2D) NMR inverse C-H correlation technique such as gradient heteronuclear multiple-bond correlation (gHMBC; $^1\text{J}_{\text{C-H}}$ with $n = 2, 3$) was used to observe the carbonyl carbon peak with respect to the proton peak in the spectra and thereby confirm the structure of intermediate I. As previously reported in the literature, gHMBC spectra can help determine long-range or multiple-bond correlation, *i.e.*, the correlation between a given carbon and the protons on the nearest two or three neighboring carbon atoms.^{21, 25} According to the ^1H NMR spectra, some portion of the α -proton peak from octylamine ($\text{NH}_2\text{CH}_2\text{C}_7\text{H}_{15}$) migrated from 2.7 ppm to 3.4 ppm because a small quantity of coordinated octylamine acted as a nucleophile to attack the electron-deficient carbon of the oleate ligand. As a result, some of the carbonyl carbon peak ($\text{Cd}(\text{CO}_2(\text{CH}_2)_7\text{CH}=\text{CH}(\text{CH}_2)_7\text{CH}_3)_2$) in ^{13}C NMR also shifted from 181.6 to 163.2 ppm as intermediate I (tetravalent carbonyl carbon) was generated. Although the actual amount of intermediate I in the NMR

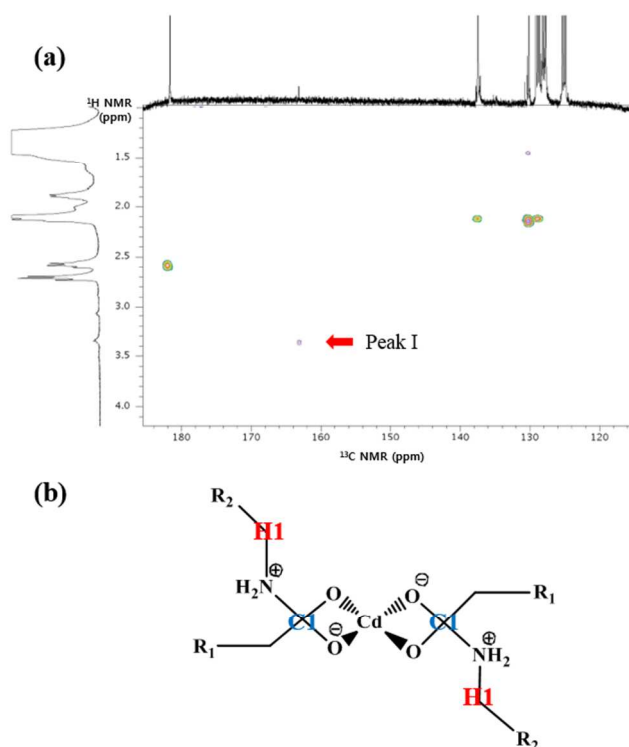


Fig. 4 NMR spectra of intermediate I, in which the octylamine migrated to the carbonyl carbon of Cd(oleate)₂ in the presence of octylamine in toluene-*d*₈; (a) peak I from 2D NMR (gHMBC) and (b) molecular structure of intermediate I

sample was not high, as shown in Fig. 2b, and its isolation was impossible, a cross-peak was clearly observed in the gHMBC spectra of intermediate I (Fig. 4a). This peak was due to long-range coupling between the carbonyl carbon of oleate and the proton of the octylamine moieties, showing a cross-peak I due to C1-H1 correlation between the carbonyl carbon (163.2 ppm) and the $-\text{NH}_2\text{CH}_2(\text{CH}_2)_6\text{CH}_3$ group (3.4 ppm) in the structure of intermediate I, as described in Fig. 4b.

When the Cd(oleate)₂ was heated to 320 °C in a non-coordinating solvent, such as octadecene, the color of the solution slowly turned brown and water was generated, which could be easily observed as being refluxed and splashed over the high boiling octadecene. After approximately 30 min at this high temperature, yellowish brown precipitates were formed, similar to those reported for Fe(oleate)₃.³⁰ Several other metal oleate complexes also thermally decomposed at 320 °C to produce the corresponding metal oxide nanoparticles, but Zn(oleate)₂ and Mn(oleate)₂ did not decompose at 320 °C. However, as shown in Fig. S1, when the same complexes were heated in the presence of an alkylamine, such as octylamine, all decomposed to produce the corresponding metal oxides, even at a lower temperature of approximately 270-280 °C; this result is similar to that reported for metal or metal sulfide nanoparticle synthesis, which showed that amines could reduce the required reaction temperature by approximately 50-100 °C.³¹⁻³⁴

To analyse the products after the thermal decomposition of the metal precursors, Cd(oleate)₂ in the presence of octylamine was heated at 250 °C for 30 min; the colorless solution turned brown upon heating, gas was evolved, and a brown precipitate formed. The precipitate was separated by centrifugation and confirmed to be cubic structured CdO nanocrystals with an average size of approximately 100 nm by powder X-ray diffraction (JCPDS: 05-0640) and SEM (Fig. 5a and 5b). The major organic side product concentrated from the supernatant

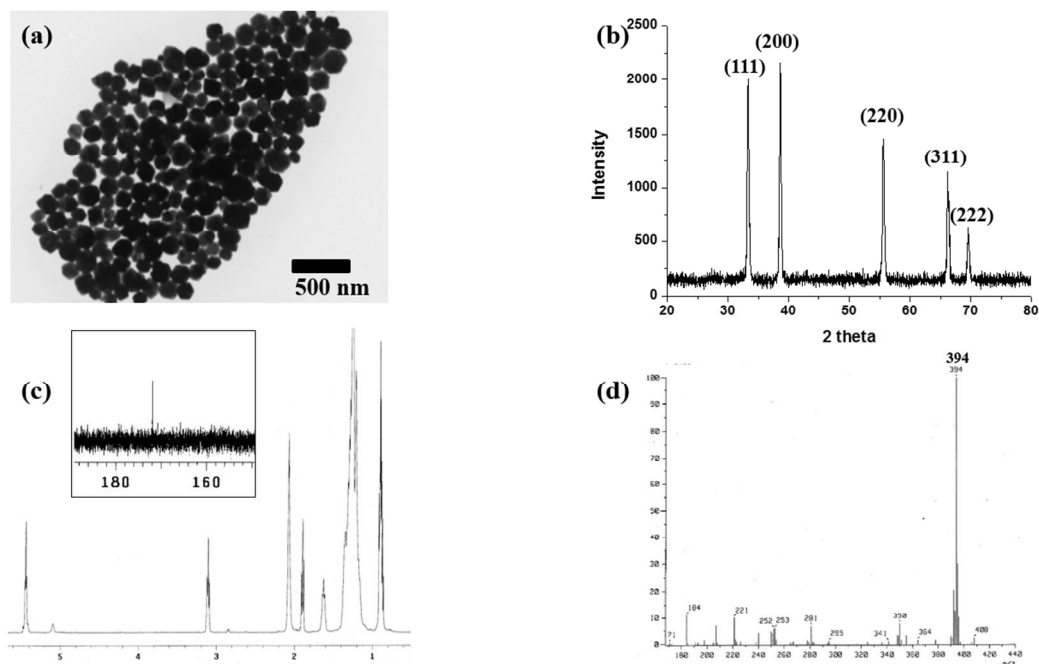


Fig. 5 (a) SEM image and (b) XRD pattern of the CdO nanoparticles. (c) ¹H-NMR (insert ¹³C-NMR) in toluene-*d*₈, (d) FAB-MS of *N*-octyloleamide synthesized from Cd(oleate)₂ and octylamine

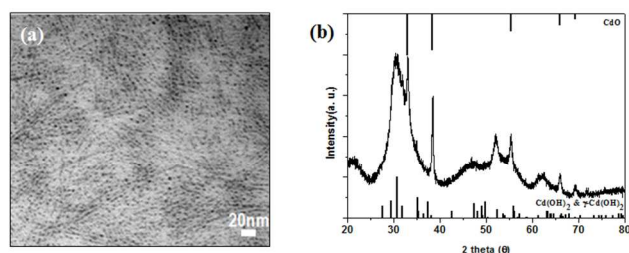


Fig. 6 (a) TEM image and (b) XRD pattern of separated intermediate II

was characterized as *N*-octyloleamide, $\text{CH}_3(\text{CH}_2)_7\text{CH}=\text{CH}(\text{CH}_2)_7\text{CO}_2\text{-NH}(\text{CH}_2)_7\text{CH}_3$, by ^1H and ^{13}C NMR spectroscopy; proton peaks from the double bonds in the oleate and octylamine units were detected at 5.42 ppm and 3.1 ppm, respectively, in toluene- d_8 , and an amide carbonyl carbon peak was clearly detected at 171.9 ppm in ^{13}C -NMR (Fig. 5c). Fast-atom-bombardment MS (FAB-MS) analysis of the isolated organic side product also confirmed the generation of *N*-octyloleamide, showing a molecular ion peak (M^+) at $m/z = 394$ (Fig. 5d). The water generated during the reaction was identified by observing the color change of cobalt chloride, which was absorbed onto paper and exposed to the water vapor inside the refluxing condenser (see Supporting Information Fig. S2).

These results show that the initial decomposition of the $\text{Cd}(\text{oleate})_2$ followed a thermal decomposition pathway similar to that of zinc bis(dimethylthiocarmate) ($\text{Zn}(\text{DMTC})_2$) in the presence of alkylamine,²⁵ where nucleophilic attack of the coordinated alkylamine of the metal center on the electron-deficient carbon of the ligand is the initial step of the thermal decomposition to generate ZnS nanoparticles and thiourea.

To analyse the thermal decomposition product of $\text{Cd}(\text{oleate})_2$ at the moment of selenium injection, the mixture of $\text{Cd}(\text{oleate})_2$ with octylamine was heated in 1-octadecene (ODE). When the temperature approached 250 °C, the solution was cooled to room temperature, and the precipitate was separated by adding an excess amount of acetone and by centrifugation. The precipitate was found to comprise very small size (< 5 nm) particles of CdO and $\text{Cd}(\text{OH})_2$ by TEM and powder X-ray diffraction analysis (Fig. 6); partially decomposed HO-CdL_n was also included in the precipitate from the pyrolysis of $\text{Cd}(\text{oleate})_2$ and octylamine to release *N*-octyloleamide. Upon further decomposition and bimolecular condensation of HO-CdL_n , Cd-O-Cd linkages were formed through the release of

H_2O , similar to the generation H_2S gas in the thermal decomposition of $\text{Zn}(\text{DMTC})_2$ with octylamine.²⁶ Because $\text{Cd}(\text{OH})_2$ could be thermally condensed to produce CdO above 170 °C,³⁵ it was reasonable to consider CdO as a major cluster (or oligomer, intermediate II) that was produced from $\text{Cd}(\text{oleate})_2$ at temperatures above 250 °C.

High quality CdSe quantum dots (QDs) approximately 4 nm in size could be synthesized from the separated intermediate II (CdO cluster as shown in Fig. 6) by dispersing it in ODE, heating to 250 °C, and injecting TOPSe, as shown in Fig. 7 (QDs were isolated at 1 min after the TOPSe injection). The absorbance and photoluminescence wavelengths of the synthesized QDs increased exponentially within 2–3 min and slowly shifted to longer wavelengths, most likely due to Ostwald ripening (see Supporting Information Fig. S3). For comparison with intermediate II, CdSe QDs were also synthesized from bulk CdO powder (325 mesh powder, Alfa Aesar) and CdO nanoparticles (~100 nm) prepared from $\text{Cd}(\text{oleate})_2$, as shown in Fig. 5a. Interestingly, the QDs synthesized from bulk CdO showed a much narrower size-distribution, as reported in the literature,²⁷ while those synthesized from 100 nm CdO nanoparticles showed a very broad size distribution (see Supporting Information Fig. S4), emphasizing the effect of the concentration of the CdO oligomer (cluster) generated from the surface of CdO that reacts with TOPSe; the amount of CdO cluster generated from 100 nm CdO nanoparticles should be higher due to the large surface area and cause the uncontrolled seed formation and growth rate to give rise to the broad size distribution.

To verify that a two-step sequential reaction occurred during the synthesis of the CdSe QDs, the possibility of the direct interaction of TOPSe with $\text{Cd}(\text{oleate})_2$ was investigated; this reaction has been suggested in the literature to dominate when no alkylamine is incorporated.^{18–23} First, the relative coordinating ability of TOPSe to $\text{Cd}(\text{oleate})_2$ compared to alkylamine was investigated, which could affect the decomposition processes. It should be mentioned that high purity TOP (97%) was purchased, and dioctylphosphine impurities were removed by vacuum distillation due to the lower boiling point of the impurities as described in the literature.³⁶ As shown in Fig. 1, the chemical shift of the α -protons in the coordinated octylamine ($\text{NH}_2\text{CH}_2(\text{CH}_2)_6\text{CH}_3$) shifted downfield from that of free octylamine (the δ of free octylamine in toluene is 2.47 ppm) due to the coordination on the metal site of $\text{Cd}(\text{oleate})_2$. When different amount of TOPSe

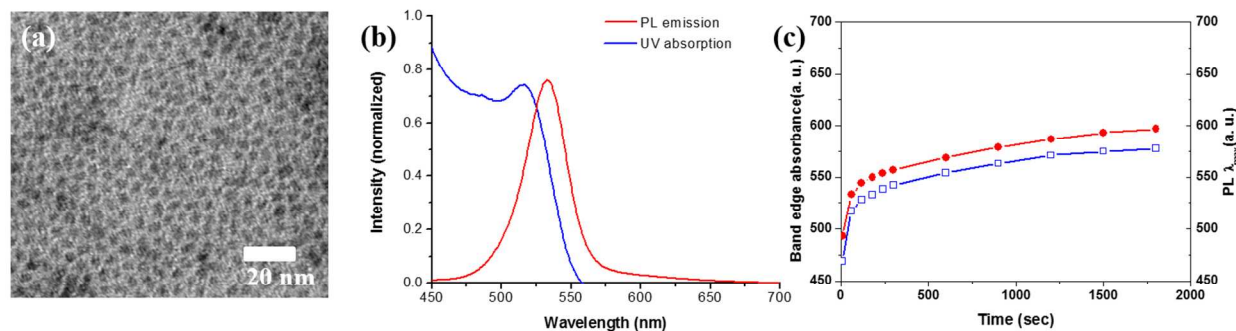


Fig. 7 (a) TEM image and (b) absorption and emission spectra of CdSe isolated at 1 min; (c) plot of band edge absorbance and PL wavelength (λ_{max}) as a function of reaction time

were added to the mixture of Cd(oleate)₂ and octylamine under the same conditions used in Fig. 1, the chemical shift of the α -protons in octylamine was monitored by ¹H NMR; 1.0 mmol of Cd(oleate)₂ and 2.0 mmol of octylamine in 10 mL of toluene-*d*₈ was mixed with 1.0 mL or 5.0 mL of TOPSe solution (1.0 mmol Se/1.0 mL TOP). Although the chemical shifts for the α -protons in octylamine (NH₂CH₂(CH₂)₆CH₃) and for the oleate ligands in Cd(oleate)₂ (Cd(CO₂CH₂(CH₂)₆CH=CH(CH₂)₇CH₃)₂) were not significantly shifted after the addition of 1.0 mmol of TOPSe, it was clearly observed that amine peak was shifted upfield to that of the free amine after the addition of 5.0 mmol of TOPSe. However, the positions and difference between those two peaks also changed slightly (marked with colour arrows in Supporting Information Fig. S5), most likely due to the solvent effect of the added TOP with TOPSe.

In order to check the relative coordination ability of TOPSe and octylamine towards Cd(oleate)₂ at higher temperature than room temperature, the changes of PL emission of the mixtures of TOPSe and Cd(Oleate)₂ with or without containing octylamine (1:1:0 or 1:1:4 molar ratio) were monitored by taking aliquots during the heating from 90 to 200 °C with the heating rate of 2 °C/min (see Supporting Information Fig. S6). When the mixture was heated without octylamine, the emission appeared at 435 nm even before the temperature reached to 90 °C and the λ_{max} increased gradually; supporting that TOPSe could directly interact with Cd(oleate)₂ at relatively low temperature to generate CdSe QDs as García-Rodríguez et al. reported.²⁴ However, when the mixture was heated with octylamine, no significant emission was observed at the temperature below 130 °C and it started to increase drastically. In addition, the emission intensity of generated CdSe QDs with octylamine was about three times larger than that of QDs generated without octylamine. These observations confirmed that the alkylamine could more strongly coordinate to the metal site of Cd(oleate)₂ than could TOPSe; therefore, the direct interaction of TOPSe with Cd(oleate)₂ was not significant in our system.

Because TOPSe did not decompose at 250 °C (without metal precursor) and the only observable phosphorous-containing product was TOPO when TOPSe was reacted with bulk CdO powder at 250 °C, as shown in Fig. S7, it was proposed that the CdO cluster or oligomer generated in the Step I, (CdO)_n, directly reacted with TOPSe to produce CdSe QDs, as shown in Step II in Scheme 1. The main driving force of Step II could be the formation of thermodynamically more stable products of CdSe and TOPO; the bond dissociation energy of Cd-Se (310 kJ/mol) is larger than that of Cd-O (142 kJ/mol), and that of P-O (596.6 kJ/mol) is larger than that of P-Se (363 kJ/mol). Therefore, the reaction of CdO and TOPSe to form CdSe and TOPO is thermodynamically very favorable ($\Delta G \cong 400$ kJ/mol), which was demonstrated by the reaction of TOPSe with bulk CdO powder.

Conclusions

We systematically investigated the thermal decomposition of Cd(oleate)₂ in the presence of alkylamine as well as the generation of CdSe QDs in order to understand the early stage formation mechanism of QDs. The decomposition mechanism of the Cd(oleate)₂ precursor molecule was similar to that of metal alkyldithiocarbamate complexes;²⁵ nucleophilic attack of

the coordinated alkylamine to the most electron-deficient carbonyl carbon of the oleate ligands in Cd(oleate)₂ initiated the decomposition to generate CdO clusters (intermediate II), which have also been shown to be stable species.^{37, 38} CdO clusters are the key material in our proposed mechanism for CdSe QD formation by reaction with TOPSe. Our results were consistent with the previously reported observation that bulk CdO powder can react with TOPSe at high temperatures to yield high quality CdSe QDs.²⁷

As a formation mechanism of CdSe QDs complementary to the mechanism that involves the direct interaction of TOPSe and/or dioctylphosphine selenide (DOPSe) with Cd(oleate)₂,¹⁸⁻²³ the critical role of alkylamines as nucleophiles in the thermolysis process and the metathesis reaction between the generated CdO cluster and TOPSe to form more stable CdSe and TOPO was suggested. Moreover, the proposed mechanism of the nucleophile-promoted thermal decomposition of M(oleate)_n precursor complexes could be extended to the synthesis of various metal-oxide and metal-chalcogenide nanoparticles from other metal precursor complexes.

Acknowledgements

This work was partially supported by the Nano R&D Program (2012-0006209) through the National Research Foundation of Korea (NRF) funded by the Ministry of Education, Science, and Technology of Korea. The authors thank Mr. J. Jo for help with the NMR experiments and Mr. J.-J. Koo for characterizing the Cd(oleate)₂ complexes. T. Kim and Y. K. Jung are grateful for the award of the BK21 fellowship.

Notes

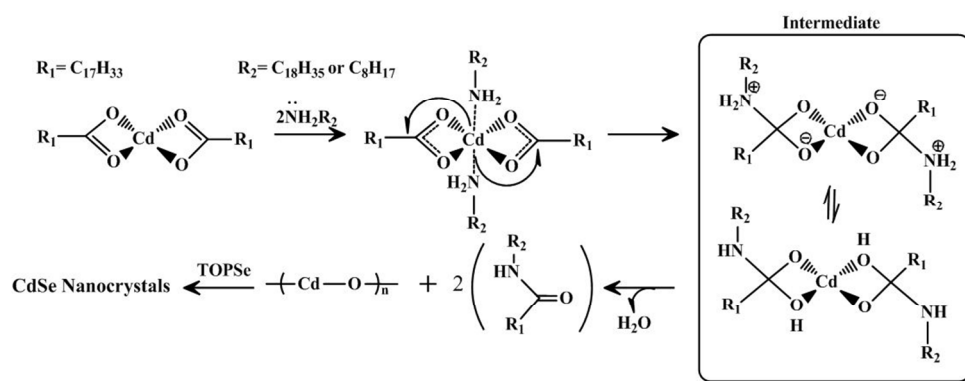
^a Department of Chemistry, Seoul National University, Seoul 151-747, South Korea. E-mail: jinklee@snu.ac.kr

† Electronic Supplementary Information (ESI) available: : TEM images and XRD patterns of various metal oxide nanoparticles; detection of water generated during the reaction; absorption and emission spectra of synthesized CdSe QDs using nano-sized CdO and bulk CdO; NMR data. See DOI: 10.1039/b000000x/

References

1. C. B. Murray, D. J. Norris and M. G. Bawendi, *J. Am. Chem. Soc.*, 1993, **115**, 8706-8715.
2. J. Y. Kim, O. Voznyy, D. Zhitomirsky and E. H. Sargent, *Adv. Mater.*, 2013, **25**, 4986-5010.
3. R. Rossetti, S. Nakahara and L. E. Brus, *J. Chem. Phys.*, 1983, **79**, 1086-1088.
4. W. W. Yu and X. G. Peng, *Angew. Chem. Int. Ed.*, 2002, **41**, 2368-2371.
5. T. Trindade and P. O'Brien, *Adv. Mater.*, 1996, **8**, 161-&.
6. Z. A. Peng and X. G. Peng, *J. Am. Chem. Soc.*, 2001, **123**, 183-184.
7. N. Pradhan and S. Efrima, *J. Am. Chem. Soc.*, 2003, **125**, 2050-2051.
8. L. Manna, E. C. Scher, L.-S. Li and A. P. Alivisatos, *J. Am. Chem. Soc.*, 2002, **124**, 7136-7145.
9. X. Peng, M. C. Schlamp, A. V. Kadavanich and A. P. Alivisatos, *J. Am. Chem. Soc.*, 1997, **119**, 7019-7029.
10. L. Manna, E. C. Scher and A. P. Alivisatos, *J. Am. Chem. Soc.*, 2000, **122**, 12700-12706.

11. B. L. Cushing, V. L. Kolesnichenko and C. J. O'Connor, *Chem. Rev.*, 2004, **104**, 3893-3946.
12. X. G. Peng, L. Manna, W. D. Yang, J. Wickham, E. Scher, A. Kadavanich and A. P. Alivisatos, *Nature*, 2000, **404**, 59-61.
13. Y. Yin and A. P. Alivisatos, *Nature*, 2005, **437**, 664-670.
14. T. Hyeon and S. G. Kwon, *Acc. Chem. Res.*, 2008, **41**, 1696-1709.
15. V. K. Lamer and R. H. Dinegar, *J. Am. Chem. Soc.*, 1950, **72**, 4847-4854.
16. D. V. Talapin, A. L. Rogach, M. Haase and H. Weller, *J. Phys. Chem. B*, 2001, **105**, 12278-12285.
17. D. V. Talapin, A. L. Rogach, E. V. Shevchenko, A. Kornowski, M. Haase and H. Weller, *J. Am. Chem. Soc.*, 2002, **124**, 5782-5790.
18. J. S. Steckel, B. K. H. Yen, D. C. Oertel and M. G. Bawendi, *J. Am. Chem. Soc.*, 2006, **128**, 13032-13033.
19. H. T. Liu, J. S. Owen and A. P. Alivisatos, *J. Am. Chem. Soc.*, 2007, **129**, 305-312.
20. J. S. Owen, E. M. Chan, H. Liu and A. P. Alivisatos, *J. Am. Chem. Soc.*, 2010, **132**, 18206-18213.
21. R. Garcia-Rodriguez and H. T. Liu, *J. Am. Chem. Soc.*, 2012, **134**, 1400-1403.
22. K. Yu, X. Y. Liu, Q. Zeng, D. M. Leek, J. Y. Ouyang, K. M. Whitmore, J. A. Ripmeester, Y. Tao and M. L. Yang, *Angew. Chem. Int. Ed.*, 2013, **52**, 4823-4828.
23. K. Yu, X. Y. Liu, Q. Zeng, M. L. Yang, J. Y. Ouyang, X. Q. Wang and Y. Tao, *Angew. Chem. Int. Ed.*, 2013, **52**, 11034-11039.
24. R. Garcia-Rodriguez and H. T. Liu, *J. Am. Chem. Soc.*, 2014, **136**, 1968-1975.
25. Y. K. Jung, J. I. Kim and J.-K. Lee, *J. Am. Chem. Soc.*, 2010, **132**, 178-184.
26. J. H. Gao, B. Zhang, Y. Gao, Y. Pan, X. X. Zhang and B. Xu, *J. Am. Chem. Soc.*, 2007, **129**, 11928-11935.
27. Z. Q. Yang, S. Cingarapu and K. J. Klabunde, *Chem. Phys. Lett.*, 2009, **470**, 112-115.
28. T. Hyeon, J. Park, K. J. An, Y. S. Hwang, J. G. Park, H. J. Noh, J. Y. Kim, J. H. Park and N. M. Hwang, *Nat. Mater.*, 2004, **3**, 891-895.
29. J. Il Kim and J. K. Lee, *Adv. Funct. Mater.*, 2006, **16**, 2077-2082.
30. J. Park, K. J. An, Y. S. Hwang, J. G. Park, H. J. Noh, J. Y. Kim, J. H. Park, N. M. Hwang and T. Hyeon, *Nat. Mater.*, 2004, **3**, 891-895.
31. H. Hiramatsu and F. E. Osterloh, *Chem. Mater.*, 2004, **16**, 2509-2511.
32. H. Khurshid, V. Tzitzios, W. F. Li, C. G. Hadjipanayis and G. C. Hadjipanayis, *J. Appl. Phys.*, 2010, **107**.
33. M. Nakamoto, M. Yamamoto and Y. Kashiwagi, *Langmuir*, 2006, **22**, 8581-8586.
34. D. L. Peng, Y. Z. Chen, D. P. Lin and X. H. Luo, *Nanotechnology*, 2007, **18**.
35. Srivasta.Ok and E. A. Secco, *Can. J. Chem.*, 1967, **45**, 1375-1378.
36. C. M. Evans, M. E. Evans and T. D. Krauss, *J. Am. Chem. Soc.*, 2010, **132**, 10973-10975.
37. R. Srinivasaraghavan, R. Chandiramouli, B. G. Jeyaprakash and S. Seshadri, *Spectrochim. Acta. A*, 2013, **102**, 242-249.
38. X. L. Cheng, F. Li and Y. Y. Zhao, *J. Mol. Struct.:Theochem*, 2009, **894**, 121-127.



267x110mm (110 x 110 DPI)